

A high-order non-oscillatory central scheme with non-staggered grids for hyperbolic conservation laws

Mehdi Dehghan*, Rooholah Jazlanian

Department of Applied Mathematics, Faculty of Mathematics and Computer Science, Amirkabir University of Technology, No. 424, Hafez Ave., Tehran, Iran

ARTICLE INFO

Article history:

Received 23 March 2010

Received in revised form 23 January 2011

Accepted 1 March 2011

Keywords:

Central scheme

Hyperbolic conservation laws

Non-linear limiters

Non-oscillatory scheme

Non-staggered grids

ABSTRACT

In this work, we present a scheme which is based on non-staggered grids. This scheme is a new family of non-staggered central schemes for hyperbolic conservation laws. Motivation of this work is a staggered central scheme recently introduced by A.A.I. Peer et al. [A new fourth-order non-oscillatory central scheme for hyperbolic conservation laws, Appl. Numer. Math. 58 (2008) 674–688]. The most important properties of the technique developed in the current paper are simplicity, high-resolution and avoiding the use of staggered grids and hence is simpler to implement in frameworks which involve complex geometries and boundary conditions. Numerical implementation of the new scheme is carried out on the scalar conservation laws with linear, non-linear flux and systems of hyperbolic conservation laws. The numerical results confirm the expected accuracy and high-resolution properties of the scheme.

© 2011 Elsevier B.V. All rights reserved.

1. Introduction

Hyperbolic systems of conservation laws arise in many practical problems such as compressible gas dynamics, shallow water flow, weather prediction, plasma modeling, and many others. For more descriptions see [23,28]. Analytical solutions are available only in very few special cases. Therefore, the numerical solution of hyperbolic systems of conservation laws has been a field of research for the last decades. It is well known that the solutions of hyperbolic conservation laws may develop discontinuities in finite time even when the initial condition is smooth.

In this paper, we present a non-oscillatory central scheme for the approximate solution of non-linear of hyperbolic conservation laws. The feature of scheme is the use of regular, non-staggered spatial grids.

The most popular methods for non-linear conservation laws are finite-volume methods and, in particular, Godunov-type schemes. These schemes form a class of projection–evolution methods, in which a computed solution is first interpolated by a piecewise polynomial function and then evolved to the next time level according to the integral form of the conservation law.

Among Godunov methods, we distinguish between *upwind* and *central* schemes. As is said in [30] the evolution step of upwind schemes is based on solvers of the Riemann problem. On the contrary, central schemes are based on the integration of conservation laws over the space–time control volumes that are selected so that each Riemann fan is entirely contained in its own control volume,

thus, no Riemann problem solver is needed. The prototype of upwind schemes is first-order upwind, which is first-order Godunov method [8], based on the solution of the Riemann problem at cell edges. The first-order Lax–Friedrichs (LxF) scheme [6] is a prototype of central schemes. Like the Godunov method, it is based on piecewise constant approximate solution and its Riemann-solver-free. As is said in [11] unfortunately, the excessive numerical viscosity in the LxF scheme yields a relatively poor resolution, which seems to have delayed the development of a high-resolution central scheme, parallel to the earlier developments of high-resolution upwind schemes.

Generally speaking, upwind schemes guarantee sharper resolution than central schemes for the same order of accuracy and grid spacing, but are more expensive, and more complicated to be implemented. For this reason, in recent years, central schemes have mostly utilized and got considerable attention.

As it is mentioned, the resolution of the LxF scheme is quite low. The performance of the LxF scheme has been enhanced in [19]. This scheme known as the NT scheme. The NT scheme is based on the reconstruction of piecewise linear polynomial from the known staggered cell-averages, and uses non-linear limiters to prevent oscillations. This scheme was extended to several space dimensions [12]. The NT scheme conserves Riemann-solver-free and hence it is simple to be implemented. Another approach to second-order central differencing based on characteristics tracing was proposed by Sander and Weiser [24]. Modifications to the NT scheme were proposed by Kurganov and Tadmor [10]. These schemes include the major advantages of the central schemes over the upwind, first: Riemann-solver-free, second: extension to multi-dimensional problem are considerably simpler than in the upwind

* Corresponding author.

E-mail addresses: mdehghan@aut.ac.ir, mdehghan.aut@gmail.com (M. Dehghan), rjazlanian@aut.ac.ir (R. Jazlanian).

case. We refer the interested reader to Refs. [9,15] and [16], for more research works on multi-dimensional conservation laws.

A third-order central scheme was proposed by Liu and Tadmor [18]. This scheme is based on the non-oscillatory third-order reconstruction of Liu and Osher [17]. The proposed scheme by Liu and Tadmor can be viewed as natural next step in the sequel to the LxF scheme, and NT scheme. This scheme has a major advantage of the central schemes [3–5] over the upwind schemes, in that no Riemann solvers are involved.

In this paper, we transform a fourth-order central scheme based on staggered grids that was proposed by Peer et al. [20] into a fourth-order central scheme based on non-staggered grids. In order to do that, we reaverage the reconstructed values of the staggered scheme. Here, we maintain the original high-resolution without giving up simplicity, and like the former scheme, the non-staggered central scheme is Riemann-solver-free. The main property of non-staggered schemes is the further simplicity since they avoid the need to alternate between two staggered grids, which is particularly a challenge near the boundaries.

This paper is organized as follows: In Section 2 we give a brief review of Godunov methods for one-dimensional hyperbolic conservation laws and fourth-order staggered central scheme of [20]. In Section 3 we describe a fourth-order non-staggered central scheme for hyperbolic conservation laws. Finally in Section 4 we test the fourth-order central scheme with staggered and non-staggered on the scalar equations and on the Euler equations.

2. One-dimensional central schemes

We approximate the solution of hyperbolic conservation laws in the form of

$$u_t + f(u)_x = 0 \tag{1}$$

with initial condition $u(x, 0) = u_0(x)$. The Godunov central schemes have two main ingredients:

1. A non-oscillatory piecewise polynomial is reconstructed from cell-averages.
2. The evolution of these reconstructed polynomials are realized at the next time level.

2.1. Non-oscillatory reconstruction

Using the formulation in [1,20] we consider a uniform spatial grid where the cell $I_x = [x - \frac{\Delta x}{2}, x + \frac{\Delta x}{2}]$ has a width Δx . Let x be the mid-cell grid point of I_x , also let $t^{n+1} = t^n + \Delta t$ and denote $u(x_j, t^n)$ by u_j^n . Let the approximation to the cell averages of u on $I_j := I_{x_j}$ and $I_{j+\frac{1}{2}} := I_{x_{j+\frac{1}{2}}}$ be given by

$$\bar{u}_j^n = \frac{1}{\Delta x} \int_{I_j} u(x, t^n) dx, \quad \bar{u}_{j+\frac{1}{2}}^n = \frac{1}{\Delta x} \int_{I_{j+\frac{1}{2}}} u(x, t^n) dx.$$

Integrating (1) over I_x , we obtain

$$\bar{u}_t(x, t) + \frac{1}{\Delta x} \left[f\left(u\left(x + \frac{\Delta x}{2}, t\right)\right) - f\left(u\left(x - \frac{\Delta x}{2}, t\right)\right) \right] = 0 \tag{2}$$

($\bar{u}_t(x, t) = \frac{1}{\Delta x} \int_{I_x} u_t(\xi, t) d\xi$), now integrating (2) over $[t^n, t^{n+1}]$, we reach

$$\bar{u}(x, t^{n+1}) = \bar{u}(x, t^n) - \frac{1}{\Delta x} \int_{t^n}^{t^{n+1}} \left[f\left(u\left(x + \frac{\Delta x}{2}, t\right)\right) - f\left(u\left(x - \frac{\Delta x}{2}, t\right)\right) \right] dt. \tag{3}$$

So far, (3) is exact. The solution to (3) is now appeared at the discrete time level $t^n = n\Delta t$ by a piecewise polynomial approximation, $w(x, t^n) \sim u(x, t^n)$, which takes the form

$$w(x, t^n) = \sum_j P_j(x) \chi_j(x), \quad \chi_j(x) := 1_{I_j}.$$

Here, $P_j(x)$ is algebraic polynomial (which has to satisfy conservation, accuracy, and non-oscillatory requirements). In general, the function $w(x, t^n)$ will be discontinuous along the boundaries of each cell I_j . Sampling (3) at $x = x_{j+\frac{1}{2}}$, we obtain the new staggered cell averages, $\bar{w}_{j+\frac{1}{2}}^{n+1}$,

$$\bar{w}_{j+\frac{1}{2}}^{n+1} = \frac{1}{\Delta x} \int_{I_{j+\frac{1}{2}}} w(x, t^n) dx - \frac{1}{\Delta x} \left[\int_{t^n}^{t^{n+1}} f(w(x_{j+1}, t)) dt - \int_{t^n}^{t^{n+1}} f(w(x_j, t)) dt \right]. \tag{4}$$

The evaluation of the expressions on the right of (4) proceeds in two steps, first: Assume that the cell averages are known, $\{\bar{w}_j^n\}$, which are used to reconstruct a non-oscillatory piecewise polynomial approximation $w(x, t^n) = \sum_j P_j(x) \chi_j(x)$.

Remark. Degree of $P_j(x)$ is determined with accuracy requirement of method. For example, a piecewise linear polynomial is used in the second-order case [19], a piecewise quadratic polynomial in third-order case [18], and a piecewise cubic polynomial in the fourth-order [20].

2.1.1. Fourth-order reconstruction with staggered grid

For the fourth-order reconstruction authors of [20] chose the cubic polynomial $P_j(x)$ on I_j in the form

$$P_j(x) = w_j^n + w_j' \left(\frac{x - x_j}{\Delta x} \right) + \frac{1}{2!} w_j'' \left(\frac{x - x_j}{\Delta x} \right)^2 + \frac{1}{3!} w_j''' \left(\frac{x - x_j}{\Delta x} \right)^3, \quad x \in I_j.$$

Here, $w_j^n, w_j'/\Delta x, w_j''/(\Delta x)^2$, and $w_j'''/(\Delta x)^3$ are the approximate point values and the first, second, and third derivatives of $w(x, t^n)$ at $x = x_j$, which are reconstructed from the cell averages, $\{\bar{w}_j^n\}$. Several approximations for these numerical derivatives are available, for further details see [18,19]. It should be noted that such reconstruction should satisfy the following three properties:

- $\mathcal{P}1$ –Conservation of cell averages: $\bar{P}_j(x)|_{x=x_j} = \bar{w}_j^n$.
- $\mathcal{P}2$ –Accuracy: $w(x, t^n) = u(x, t^n) + \mathcal{O}((\Delta x)^4)$.
- $\mathcal{P}3$ –Non-oscillatory behavior of $\sum_j P_j(x) \chi_j(x)$.

In order to guarantee property $\mathcal{P}1$, w_j^n must satisfy

$$w_j^n = \bar{w}_j^n - \frac{w_j''}{24}. \tag{5}$$

Remark. Starting with third-order and higher-order accurate methods, point values aren't equal with cell averages, $w_j^n \neq \bar{w}_j^n$.

The NT scheme uses a second-order accurate limiter for the numerical derivative w_j' in the form

$$w_j' = \mathbf{MM}(\Delta \bar{w}_{j-\frac{1}{2}}, \Delta \bar{w}_{j+\frac{1}{2}}). \tag{6}$$

Here, $\Delta \bar{w}_{j+\frac{1}{2}} = \bar{w}_{j+1} - \bar{w}_j$ and the MinMod limiter (**MM**) is defined by

$$\mathbf{MM}(x_1, x_2, \dots) = \begin{cases} \min_p \{x_p\} & \text{if } x_p > 0 \forall p \in \mathbb{N}, \\ \max_p \{x_p\} & \text{if } x_p < 0 \forall p \in \mathbb{N}, \\ 0 & \text{otherwise.} \end{cases}$$

It should be noted that the accuracy of (6) decreases when $\Delta \bar{w}_{j-\frac{1}{2}} \cdot \Delta \bar{w}_{j+\frac{1}{2}} < 0 \neq w'_j$. The NT scheme modified the uniform non-oscillatory (UNO) limiter of Harten and Osher [7] by adding second-order differences to (6) to get high accuracy

$$w'_j = \mathbf{MM} \left(\Delta \bar{w}_{j-\frac{1}{2}} + \frac{1}{2} \mathbf{MM}(\Delta^2 \bar{w}_{j-1}, \Delta^2 \bar{w}_j), \Delta \bar{w}_{j+\frac{1}{2}} - \frac{1}{2} \mathbf{MM}(\Delta^2 \bar{w}_j, \Delta^2 \bar{w}_{j+1}) \right), \quad (7)$$

where $\Delta^2 \bar{w}_j = \Delta \bar{w}_{j+\frac{1}{2}} - \Delta \bar{w}_{j-\frac{1}{2}}$.

Authors of [20], in order to satisfy properties $\mathcal{P}2$ – $\mathcal{P}3$ utilize the modified UNO limiter of [21]. Similar to the numerical derivative (6), w'''_j depends on its two neighboring third-order differences

$$w'''_j = \mathbf{MM}(\Delta^3 \bar{w}^n_{j-\frac{1}{2}}, \Delta^3 \bar{w}^n_{j+\frac{1}{2}}), \quad (8)$$

where $\Delta^3 \bar{w}^n_{j+\frac{1}{2}} = \Delta^2 \bar{w}^n_{j+1} - \Delta^2 \bar{w}^n_j$. Similar to the UNO limiter, for obtaining fourth-order accurate approximations of the first derivative, they put

$$w'_j = \mathbf{MM} \left(\Delta \bar{w}^n_{j-\frac{1}{2}} + \frac{1}{2} \mathbf{MM} \left(\Delta^2 \bar{w}^n_{j-1} + \frac{7}{12} w'''_{j-1}, \Delta^2 \bar{w}^n_j - \frac{5}{12} w'''_j \right), \Delta \bar{w}^n_{j+\frac{1}{2}} - \frac{1}{2} \mathbf{MM} \left(\Delta^2 \bar{w}^n_j + \frac{5}{12} w'''_j, \Delta^2 \bar{w}^n_{j+1} - \frac{7}{12} w'''_{j+1} \right) \right), \quad (9)$$

for further details see [20,21]. In order to approximate the point values w^n_j of (5) from the cell averages, authors of [20], put

$$w''_j = \mathbf{MM}(\Delta^2 \bar{w}^n_{j-1} + w'''_{j-1}, \Delta^2 \bar{w}^n_j, \Delta^2 \bar{w}^n_{j+1} - w'''_{j+1}). \quad (10)$$

The staggered cell averages $\bar{w}^n_{j+\frac{1}{2}}$ which are used on the right of (4) are given by

$$\begin{aligned} \bar{w}^n_{j+\frac{1}{2}} &= \frac{1}{\Delta x} \int_{I_{j+\frac{1}{2}}} w(x, t^n) dx = \frac{1}{\Delta x} \int_{I_{j+\frac{1}{2}}} \sum_j P_j(x) \chi_j(x) dx \\ &= \frac{1}{\Delta x} \left[\int_{x_j}^{x_{j+\frac{1}{2}}} P_j(x) dx + \int_{x_{j+\frac{1}{2}}}^{x_{j+1}} P_{j+1}(x) dx \right] \\ &= \frac{1}{2} (\bar{w}^n_j + \bar{w}^n_{j+1}) - \frac{1}{8} (w'_{j+1} - w'_j) \\ &\quad - \frac{1}{384} (w'''_{j+1} - w'''_j). \end{aligned} \quad (11)$$

2.2. Staggered evolution

Here, we describe the second step in the implementation of the central scheme. The second step is the evolution of the reconstructed point values $\{w^n_j\}$. As is said in [1] if $\{a_k(u)\}$ are the

eigenvalues of the Jacobian $A(u) := \frac{\partial f}{\partial u}$, then by hyperbolicity, information regarding the interfacing discontinuities at $x_{j\pm\frac{1}{2}}$ propagates no faster than $\max_k |a_k(u)|$. Hence, the mid-cell values, $\{w^n_j\}$, remain free of discontinuities as long as the Courant–Friedrichs–Lewy (CFL) restriction, $\Delta t \leq \frac{1}{2} \max_k |a_k(u)|$, is met [1]. Then, the flux integrals in the right of (4) involve only smooth integrands and can be evaluated with proper quadrature rules to any desired degree of accuracy. For example, authors of [19] use the mid point's quadrature rule

$$\int_{t^n}^{t^{n+1}} f(w(x_j, t)) dt = \Delta t f(w(x_j, t^{n+\frac{1}{2}})) + \mathcal{O}((\Delta t)^2),$$

while the third-order Liu–Tadmor scheme [18] and the fourth-order scheme of Peer et al. [20] employ the Simpson's rule

$$\int_{t^n}^{t^{n+1}} f(w(x_j, t)) dt = \frac{\Delta t}{6} [f(w(x_j, t^n)) + 4f(w(x_j, t^{n+\frac{1}{2}})) + f(w(x_j, t^{n+1}))] + \mathcal{O}((\Delta t)^5). \quad (12)$$

As it can be seen from these quadrature formulae, we require the computation of the intermediate point values $w_j^{n+\beta}$, $\beta = 0, \frac{1}{2}, 1$. There are various approaches for computing these intermediate point values. A first approach employs Taylor's expansion and the differential equation, $w_t = -f(w)_x$ [19]. Another approach employs Runge–Kutta solvers of the Ordinary Differential Equation (ODE) $w_t = -f_x|_{x=x_j}$, $w(x_j, 0) = w^n_j$, $t > t^n$. Bianco, Puppo and Russo [2] proposed the use of Natural Continuous Extension (NCE) of Runge–Kutta (RK) schemes [29] in order to reduce the number of computations. We shall briefly describe the NCE of RK methods. We consider the Cauchy problem

$$\begin{cases} y' = F(t, y(t)), \\ y(t_0) = y_0. \end{cases}$$

The solution obtained at time t^{n+1} with a ν -step explicit RK scheme of order p can be written as

$$y^{n+1} = y^n + \Delta t \sum_{i=1}^{\nu} b_i K^{(i)},$$

where the $K^{(i)}$'s are the RK fluxes

$$K^{(i)} = F \left(t^n + \Delta t c_i, y_n + \Delta t \sum_{j=1}^{i-1} a_{ij} K^{(j)} \right), \quad c_i = \sum_{j=1}^i a_{ij}.$$

We can combine y^n, y^{n+1} and $K^{(i)}$, to obtain an extension of the numerical solution of the ODE, in the sense that, there exist ν polynomials $b_i(\theta)$ of degree $d \leq p$, such that

1. $y(t^n + \theta \Delta t) = y^n + \Delta t \sum_{i=1}^{\nu} b_i(\theta) K^{(i)}$, $0 \leq \theta \leq 1$,
2. $y(t^n) = y^n$, $y(t^n + \Delta t) = y^{n+1}$,
3. $\max_{0 \leq \theta \leq 1} |y^{(l)}(t^n + \theta \Delta t) - w^{(l)}(t^n + \theta \Delta t)| = \mathcal{O}(\Delta t^{d+1-l})$,

where $w(t)$ is the exact solution of ODE at time t^n ($w_t = -f_x|_{x=x_j}$, $w(x_j, 0) = w^n_j$, $t > t^n$). For a uniformly fourth-order accurate scheme in time, we need $d + 1 = 4$. The NCE of a fourth-order RK scheme is

$$b_1(\theta) = 2(1 - 4b_1)\theta^3 + 3(3b_1 - 1)\theta^2 + \theta,$$

$$b_i(\theta) = 4(3c_i - 2)b_i\theta^3 + 3(3 - 4c_i)b_i\theta^2, \quad i = 2, 3, 4,$$

where $c_i = \sum_j a_{ij}$ and the coefficients b_i and a_{ij} are given by

$$b = \begin{pmatrix} 1/6 \\ 1/3 \\ 1/3 \\ 1/6 \end{pmatrix}, \quad a = \begin{pmatrix} 0 & 0 & 0 & 0 \\ 1/2 & 0 & 0 & 0 \\ 0 & 1/2 & 0 & 0 \\ 0 & 0 & 1 & 0 \end{pmatrix}.$$

Here, $F(z, v_i(z)) = -\frac{1}{\Delta x} f'(v(x_i, t^n + z)) \simeq -f_x(v(x_i, t^n + z))$. Since we need to intermediate point values at time $t^{n+\frac{1}{2}}$ and t^{n+1} for computing the quadrature formula (12), we have

$$w\left(x_j, t^n + \frac{\Delta t}{2}\right) = w_j^n + \Delta t \sum_{i=1}^4 b_i \left(\frac{1}{2}\right) K^{(i)} \\ = w_j^n + \frac{\Delta t}{6} \left(\frac{5}{4} K^1 + K^2 + K^3 - \frac{1}{4} K^4\right),$$

$$w(x_j, t^n + \Delta t) = w_j^n + \Delta t \sum_{i=1}^4 b_i (1) K^{(i)} \\ = w_j^n + \frac{\Delta t}{6} (K^1 + 2K^2 + 2K^3 + K^4).$$

Here, for computing the RK fluxes, i.e. $K^{(i)}$ we need to approximate f'_j . For this purpose, similar to (9) by combining high-order differences of f put

$$f'_j = \mathbf{MM} \left(\Delta f_{j-\frac{1}{2}} + \frac{1}{2} \mathbf{MM} \left(\Delta^2 f_{j-1} + \frac{2}{3} f'''_{j-1}, \Delta^2 f_j - \frac{1}{3} f'''_j \right), \right. \\ \left. \Delta f_{j+\frac{1}{2}} - \frac{1}{2} \mathbf{MM} \left(\Delta^2 f_j + \frac{1}{3} f'''_j, \Delta^2 f_{j+1} - \frac{2}{3} f'''_{j+1} \right) \right), \quad (13)$$

where

$$f'''_j = \mathbf{MM}(\Delta^3 f_{j-\frac{1}{2}}, \Delta^3 f_{j+\frac{1}{2}}).$$

Remark. Since the derived scheme uses alternating, staggered grids, one has to distinguish between the “odd” and “even” time steps. The above formulae describe the “odd” steps. The “even” steps are obtained by shifting the indexes in the aforementioned equations by $\frac{1}{2}$. Obviously, the computational domain should be extended by $\frac{\Delta x}{2}$ from both sides at every “even” step. So, in frameworks which involve complex geometries, the imposition of boundary conditions is a complicated and tiresome work. Therefore, we are now ready to construct non-staggered version of the fourth-order staggered scheme.

3. Fourth-order non-staggered scheme

In this section, we transform the fourth-order staggered scheme into fourth-order non-staggered scheme. For this work, first, we have to reconstruct a piecewise cubic polynomial from the staggered cell averages and project it on the non-staggered cell averages,

$$w(x, t^{n+1}) := \sum_j P_{j+\frac{1}{2}}^{n+1}(x) \chi_{j+\frac{1}{2}}(x), \quad (14)$$

where $\chi_{j+\frac{1}{2}}(x) := 1_{I_{j+\frac{1}{2}}}$ and

$$P_{j+\frac{1}{2}}^{n+1}(x) = w_{j+\frac{1}{2}}^{n+1} + w'_{j+\frac{1}{2}} \left(\frac{x - x_{j+\frac{1}{2}}}{\Delta x} \right) + \frac{1}{2!} w''_{j+\frac{1}{2}} \left(\frac{x - x_{j+\frac{1}{2}}}{\Delta x} \right)^2 \\ + \frac{1}{3!} w'''_{j+\frac{1}{2}} \left(\frac{x - x_{j+\frac{1}{2}}}{\Delta x} \right)^3, \quad x \in I_{j+\frac{1}{2}}.$$

The staggered discrete derivatives, $w'_{j+\frac{1}{2}}$, $w''_{j+\frac{1}{2}}$ and $w'''_{j+\frac{1}{2}}$, are given by

$$w'''_{j+\frac{1}{2}} = \mathbf{MM}(\Delta^3 \bar{w}_j^{n+1}, \Delta^3 \bar{w}_{j+1}^{n+1}), \quad (15)$$

$$w''_{j+\frac{1}{2}} = \mathbf{MM}(\Delta^2 \bar{w}_{j-\frac{1}{2}}^{n+1} + w'''_{j-\frac{1}{2}}, \Delta^2 \bar{w}_{j+\frac{1}{2}}^{n+1}, \\ \Delta^2 \bar{w}_{j+\frac{3}{2}}^{n+1} - w'''_{j+\frac{3}{2}}),$$

$$w'_{j+\frac{1}{2}} = \mathbf{MM} \left(\Delta \bar{w}_j^{n+1} + \frac{1}{2} \mathbf{MM} \left(\Delta^2 \bar{w}_{j-\frac{1}{2}}^{n+1} + \frac{7}{12} w'''_{j-\frac{1}{2}}, \right. \right. \\ \left. \left. \Delta^2 \bar{w}_{j+\frac{1}{2}}^{n+1} - \frac{5}{12} w'''_{j+\frac{1}{2}} \right), \right. \\ \left. \Delta \bar{w}_{j+1}^{n+1} - \frac{1}{2} \mathbf{MM} \left(\Delta^2 \bar{w}_{j+\frac{1}{2}}^{n+1} + \frac{5}{12} w'''_{j+\frac{1}{2}}, \right. \right. \\ \left. \left. \Delta^2 \bar{w}_{j+\frac{3}{2}}^{n+1} - \frac{7}{12} w'''_{j+\frac{3}{2}} \right) \right). \quad (16)$$

Second, the cell averages at the next time step, \bar{w}_j^{n+1} , are obtained by averaging the piecewise cubic polynomial (14), then we have

$$\bar{w}_j^{n+1} = \frac{1}{\Delta x} \int_{I_j} w(x, t^{n+1}) dx \\ = \frac{1}{\Delta x} \left[\int_{x_{j-\frac{1}{2}}}^{x_j} P_{j-\frac{1}{2}}^{n+1}(x) dx + \int_{x_j}^{x_{j+\frac{1}{2}}} P_{j+\frac{1}{2}}^{n+1}(x) dx \right] \\ = \frac{1}{2} (w_{j+\frac{1}{2}}^{n+1} + w_{j-\frac{1}{2}}^{n+1}) - \frac{1}{8} (\tilde{w}'_{j+\frac{1}{2}} - \tilde{w}'_{j-\frac{1}{2}}) \\ + \frac{1}{48} (\tilde{w}''_{j+\frac{1}{2}} + \tilde{w}''_{j-\frac{1}{2}}) - \frac{1}{384} (\tilde{w}'''_{j+\frac{1}{2}} - \tilde{w}'''_{j-\frac{1}{2}}).$$

It should be noted that $P_{j+\frac{1}{2}}^{n+1}(x)$ should satisfy the three properties $\mathcal{P}1$ – $\mathcal{P}3$ introduced in Section 2.1.1. Then, in order to guarantee property $\mathcal{P}1$, $w_{j\pm\frac{1}{2}}^{n+1}$ must satisfy

$$w_{j\pm\frac{1}{2}}^{n+1} = \bar{w}_{j\pm\frac{1}{2}}^{n+1} - \frac{\tilde{w}''_{j\pm\frac{1}{2}}}{24},$$

therefore, we conclude that

$$\bar{w}_j^{n+1} = \frac{1}{2} (\bar{w}_{j+\frac{1}{2}}^{n+1} + \bar{w}_{j-\frac{1}{2}}^{n+1}) - \frac{1}{8} (\tilde{w}'_{j+\frac{1}{2}} - \tilde{w}'_{j-\frac{1}{2}}) \\ - \frac{1}{384} (\tilde{w}'''_{j+\frac{1}{2}} - \tilde{w}'''_{j-\frac{1}{2}}). \quad (17)$$

Here, $\{\tilde{w}'_{j\pm\frac{1}{2}}\}$ and $\{\tilde{w}''_{j\pm\frac{1}{2}}\}$ are discrete derivatives at time level t^{n+1} given in (16) and (15) respectively. Also

$$\bar{w}_{j+\frac{1}{2}}^{n+1} + \bar{w}_{j-\frac{1}{2}}^{n+1} = \frac{1}{2} (\bar{w}_{j+1}^n + 2\bar{w}_j^n + \bar{w}_{j-1}^n) - \frac{1}{8} (w'_{j+1} - w'_{j-1}) \\ - \frac{1}{384} (w'''_{j+1} - w'''_{j-1}) \\ - \frac{\lambda}{6} [f(w_{j+1}^n) + 4f(w_{j+\frac{1}{2}}^{n+\frac{1}{2}}) + f(w_{j-1}^n)] \\ - f(w_j^n) - 4f(w_{j+\frac{1}{2}}^{n+\frac{1}{2}}) - f(w_{j-1}^{n+1})].$$

Here, we combine the results of previous section with our new non-staggered central scheme of this section. The derivation of the resulting scheme is straightforward and is summarized in the following algorithm:

Assuming that the cell averages $\{\bar{w}_j^n\}$ are known, we look for the cell averages $\{\bar{w}_j^{n+1}\}$.

- Step 1. Compute the numerical derivatives w_j''', w_j'', w_j' given by (8), (10) and (9).
- Step 2. Compute the point values w_j^n with (5). Compute the intermediate point values with NCE-RK.
- Step 3. Compute the numerical derivatives at t^{n+1} with (15) and (16).
- Step 4. Compute the non-staggered cell averages \bar{w}_j^{n+1} with (17).

4. Numerical results

In this section we report the numerical results of some test problems to support our theoretical results. For this work, we compare the fourth-order staggered central scheme with the fourth-order non-staggered central scheme. The time step is determined by imposing the Courant number. Peer et al. in [20] carried out a linear stability of the central staggered scheme (4), in order to obtain its critical Courant number. For one-dimensional case the linear stability analysis carried out in [20] yields a Courant number $C = 0.3408$. We remark that the stencil used here is similar to the one that used in [20], then we put $C = 0.3408$. Let $u(x_j, t^n)$ and w_j^n be the exact solution and the reconstructed solution respectively at (x_j, t^n) . Then the norms of the error are given by:

$$L_1 \text{ error: } \|u - w\|_1 = \sum_{j=1}^N |u(x_j, t^n) - w_j^n| \Delta x,$$

$$L_\infty \text{ error: } \|u - w\|_\infty = \max_{1 \leq j \leq N} |u(x_j, t^n) - w_j^n|.$$

4.1. Scalar equation

We study the results of numerical experiments using four scalar test cases.

Test 1.

$$u_t + u_x = 0,$$

$$u(x, 0) = \sin(x), \quad x \in [0, 2\pi],$$

Periodic boundary condition
Integration time: $T = 1$.

This test is used to check the convergence rate. We solved this test with $\lambda = 0.9C$. The L_1 and L_∞ errors and orders of convergence are reported in Table 1. It can be seen that the scheme converges

Table 1
Errors and orders of convergence for Test 1.

N	L_∞ error	L_∞ order	L_1 error	L_1 order
40	2.5489(-4)	-	3.4206(-4)	-
80	2.7153(-5)	3.2307	2.3748(-5)	3.6551
160	3.1205(-6)	3.1213	1.6084(-6)	4.0774
320	3.4422(-7)	3.1804	1.0635(-7)	3.9187
640	3.7727(-8)	3.1897	6.8205(-9)	3.9628

Table 2
Errors and orders of convergence for Test 2.

N	L_∞ error	L_∞ order	L_1 error	L_1 order
Before the shock $T = 0.12$				
40	5.2290(-5)	-	2.3663(-5)	-
80	5.4708(-6)	3.2567	1.6557(-6)	3.8371
160	5.7591(-7)	3.2478	1.1141(-7)	3.8935
320	1.6329(-7)	1.8184	8.3650(-9)	3.7354
After the shock $T = 1.5$				
40	0.0681	-	0.0076	-
80	0.0730	-0.1002	0.0039	0.9625
160	0.0797	-0.1267	0.0022	0.8260
320	0.0764	0.0610	0.0014	1.1375

to fourth-order accuracy in L_1 , but converges to third-order accuracy in L_∞ as the grids are refined.

Test 2. As the second test problem we use

$$u_t + \left(\frac{1}{2}u^2\right)_x = 0,$$

$$u(x, 0) = 1 + \frac{1}{2} \sin(\pi x), \quad x \in [-1, 1],$$

Periodic boundary condition
Integration time: $T = 0.12$ and $T = 1.5$.

Here, $T = 0.12$ is chosen for convergence test, and $T = 1.5$ for shock capturing test (it should be noted that shock develops at $T_s = 2/\pi$). In this test we solve the problem with $\lambda = 0.9C$. The L_1 and L_∞ errors and orders of convergence before ($T = 0.12$) and after ($T = 1.5$) shock are shown in Table 2. The L_1 order of convergence before the shock is almost 4, whereas the L_∞ order of convergence is near to 3. Numerical results are shown in Fig. 1 at $T = 1.5$ by $N = 40$. We note that the staggered scheme yields slightly better results than the non-staggered scheme when $N = 40$.

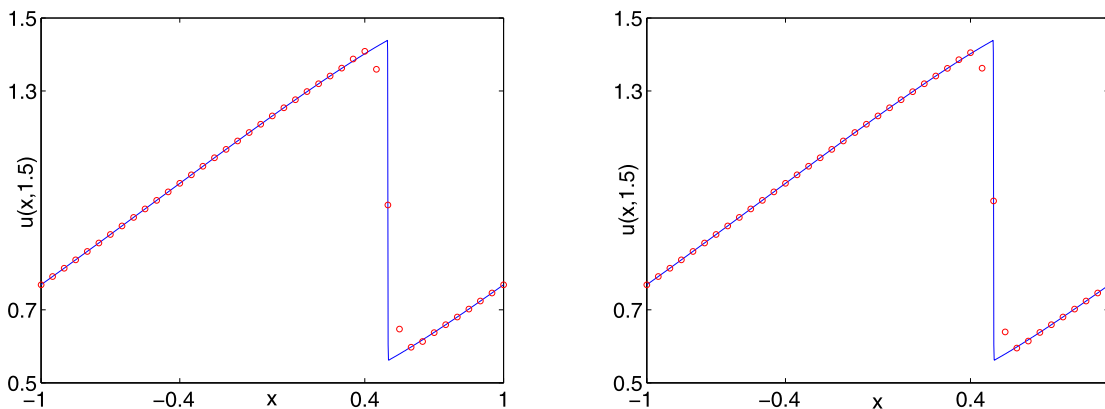


Fig. 1. Test 2 by $N = 40$ at $T = 1.5$. Left non-staggered, right staggered. -: Exact, o: approximate.

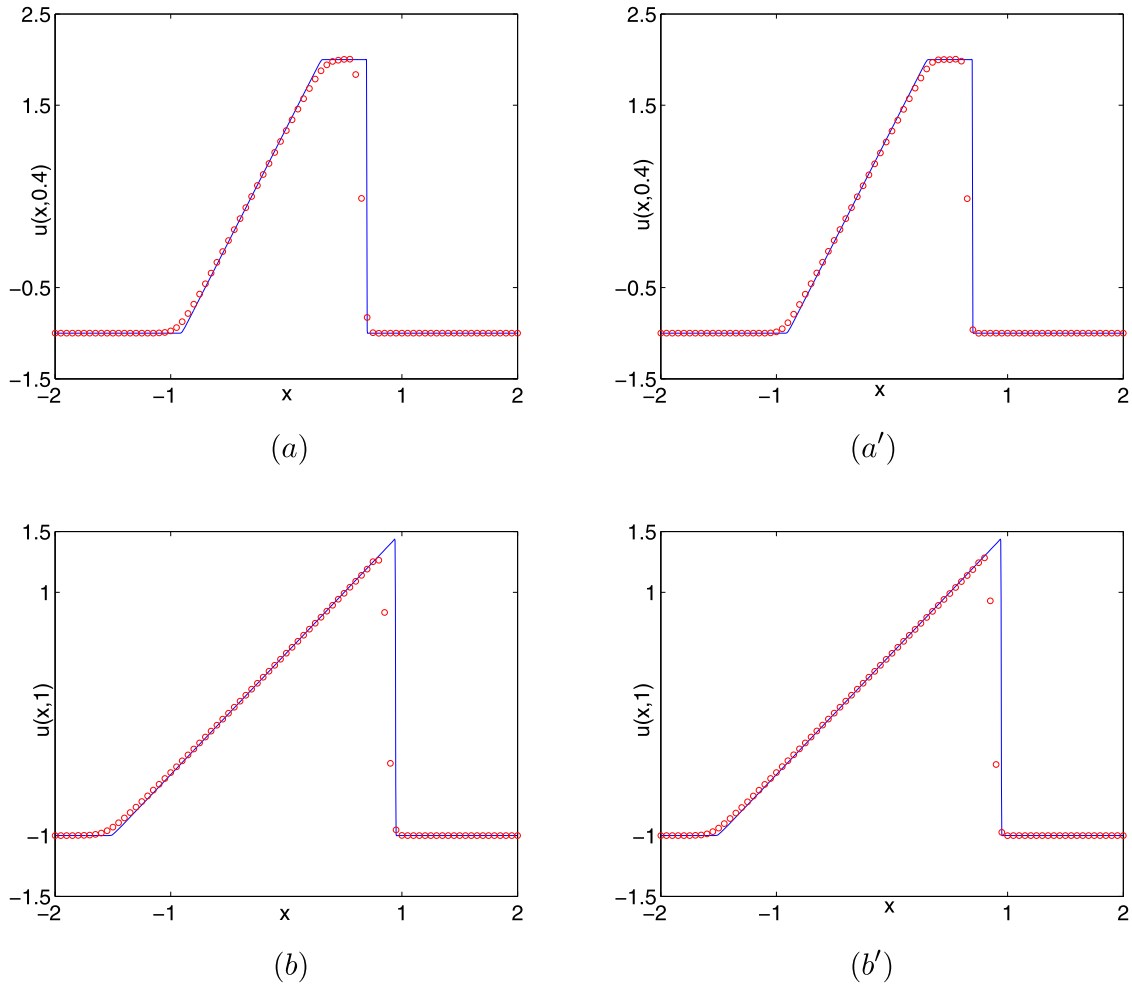


Fig. 2. Test 3 by $N = 80$ at $T = 0.4, 1$. Left non-staggered, right staggered. —: Exact, \circ : approximate. (a), (a') are before the shock and (b), (b') are after the shock.

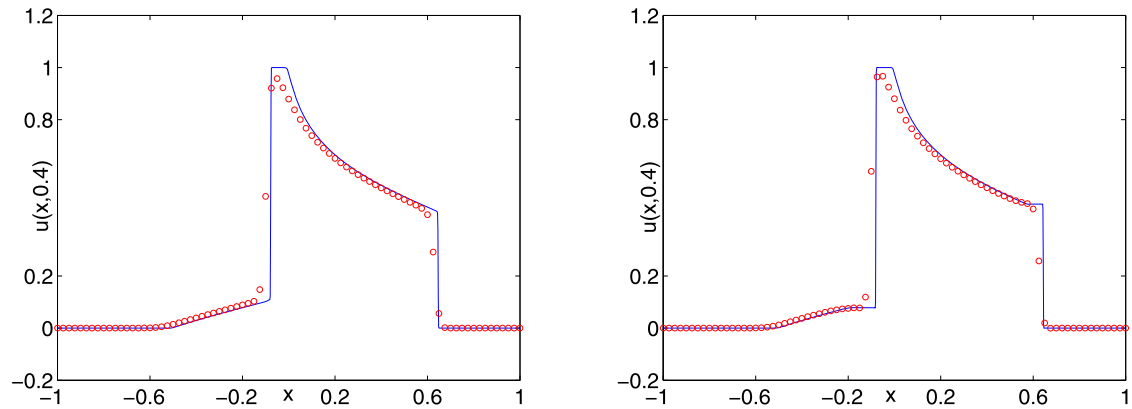


Fig. 3. Test 4 by $N = 80$ at $T = 0.4$. Left non-staggered, right staggered. —: Exact, \circ : approximate.

Test 3. Let us consider the following test

$$u_t + \left(\frac{1}{2}u^2\right)_x = 0,$$

$$u(x, 0) = \begin{cases} -1, & |x| \geq 0.5, \\ 2, & |x| < 0.5, \end{cases} \quad x \in [-2, 2],$$

Periodic boundary condition

Integration time: $T = 0.4$ and $T = 1$.

(It should be noted that shock develops at $T_s = 2/3 \simeq 0.67$.)

In this test we put $\lambda = \frac{2}{3}C$. In Fig. 2 we show the solutions at $T = 0.4$ before the shock and $T = 1$ after the shock. As expected the staggered central scheme produces slightly better results (not shown here) for all parts of the solutions while the non-staggered central scheme is well comparable with the staggered central scheme. The simplicity and efficiency of the non-staggered scheme must be noted.

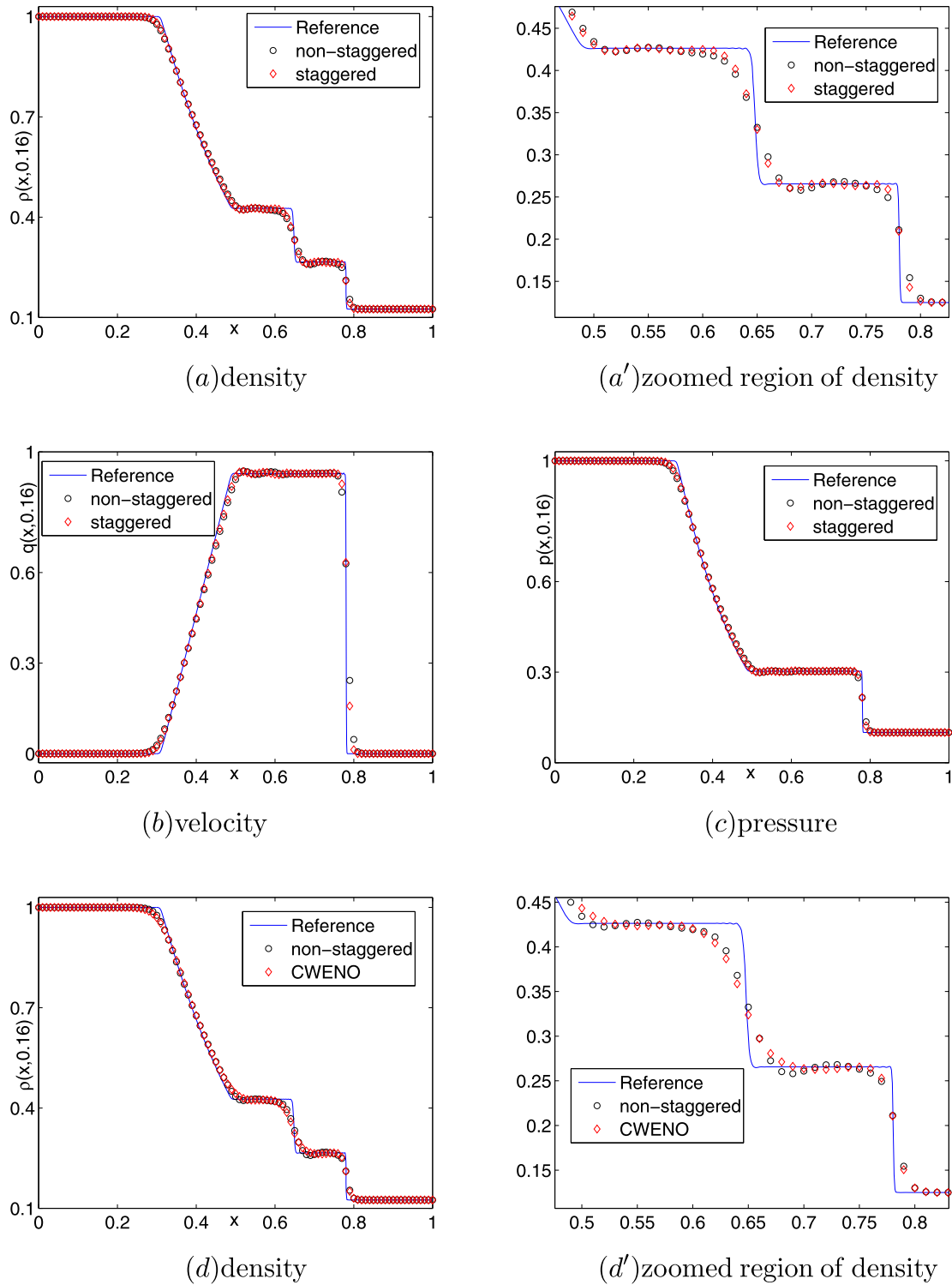


Fig. 4. Test 5 by $N = 100$ at $T = 0.16$.

Test 4 (*The Buckley–Leverett equation*). It is a non-convex problem and is given by [22].

$$u_t + \left(\frac{4u^2}{4u^2 + (1-u)^2} \right)_x = 0,$$

$$u(x, 0) = \begin{cases} 1, & -0.5 \leq x \leq 0, \\ 0, & \text{otherwise,} \end{cases} \quad x \in [-1, 1],$$

Periodic boundary condition
 Integration time: $T = 0.4$.

In this test we compute the solution at $T = 0.4$ and use the $\lambda = \frac{2}{3}C$. The exact solution is a shock–rarefaction–contact discontinuity mixture. We notice that some high-order schemes fail to converge to the correct entropy solution for this problem. The results are presented in Fig. 3. As it can be seen for all parts of the solution the non-staggered central scheme is well comparable with the staggered central scheme.

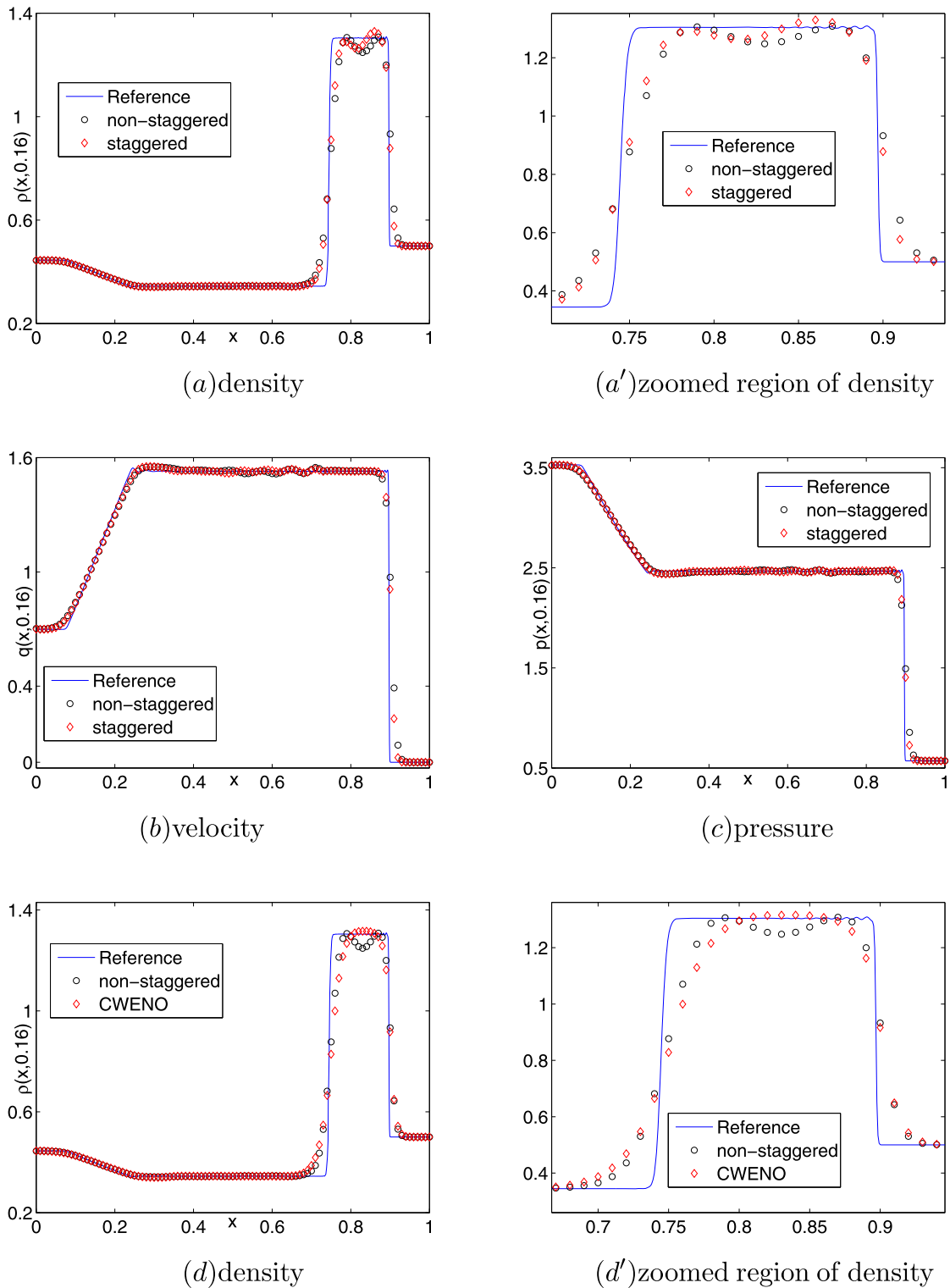


Fig. 5. Test 6 by $N = 100$ at $T = 0.16$.

4.2. Systems of equations

In this subsection we test fourth-order central schemes with staggered and non-staggered grids on the system of Euler equations for a polytropic gas, with $\gamma = 1.4$,

$$\frac{\partial}{\partial t} \begin{pmatrix} \rho \\ \rho q \\ E \end{pmatrix} + \frac{\partial}{\partial x} \begin{pmatrix} \rho q \\ \rho q^2 + p \\ q(E + p) \end{pmatrix} = 0,$$

$$p = (\gamma - 1) \left(E - \frac{1}{2} \rho q^2 \right). \tag{18}$$

Here, ρ , q , p and E are the density, velocity, pressure and total energy of the conserved fluid, respectively. Also, we compare the fourth-order non-staggered central scheme with the fourth-order staggered central weighted essentially non-oscillatory (CWENO) scheme [14]. There are various ways to extend the numerical schemes for solving hyperbolic systems of conservation laws. We

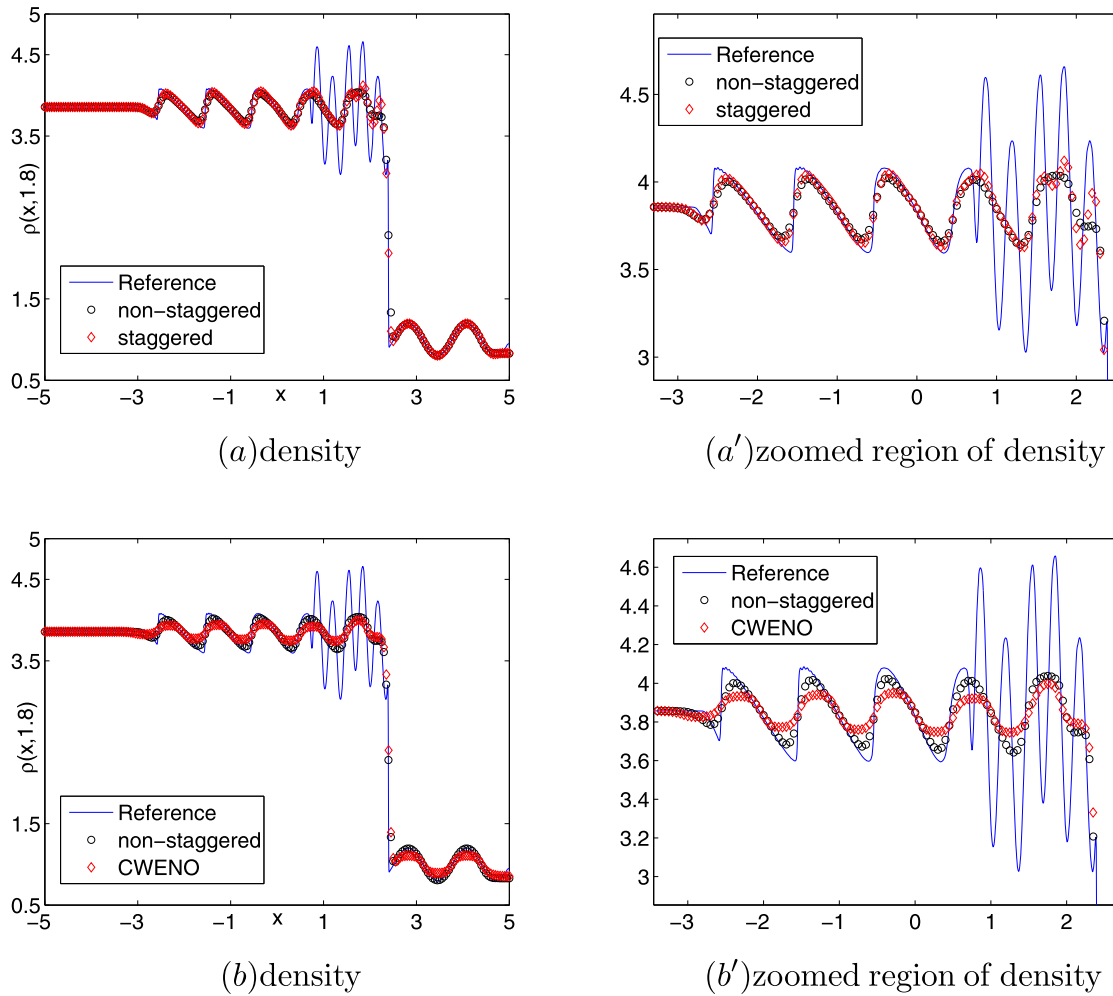


Fig. 6. Test 7 by $N = 200$ at $T = 1.8$.

shall mention two of them, the first approach is componentwise extension, also, we can utilize characteristic decomposition. In the present work, we utilize the first approach which is less costly (because we don't need the Jacobian matrix $A(u) := \frac{\partial f}{\partial u}$ and eigenstructure of the system). We choose the time step dynamically with CFL restriction

$$\Delta t = \frac{0.9C\Delta x}{\max_j(c_j + |q_j|)},$$

where c_j and q_j are the local sound speed and velocity, respectively. This time step evaluation technique can accommodate for problems where the characteristic speeds change wildly in time.

Test 5 (Sod's problem). In this test which is taken from the literature [26] we solve (18) with the initial condition and time integration:

$$u(x, 0) = \begin{cases} (1, 0, 2.5)^T, & 0 \leq x < 0.5, \\ (0.125, 0, 0.25)^T, & 0.5 \leq x \leq 1, \end{cases} \quad x \in [0, 1],$$

Integration time: $T = 0.16$.

Fig. 4 shows the performance of non-staggered, staggered grids and CWENO schemes at $T = 0.16$ with $N = 100$. Comparing the results in Fig. 4, we observe that the non-staggered central scheme is still comparable with staggered central scheme. But, the non-staggered scheme gives slightly lower resolution at the two ends of the rarefaction wave, the contact and the shock. Also, we ob-

serve in Fig. 4 that the non-staggered is sharper than CWENO in particular for the density profile of this Riemann problem.

Test 6 (Lax's problem). In this test which is taken from the literature [13] we solve (18) with the initial condition and time integration:

$$u(x, 0) = \begin{cases} (0.445, 0.31061, 8.92840289)^T, & 0 \leq x < 0.5, \\ (0.5, 0, 1.4275)^T, & 0.5 \leq x \leq 1, \end{cases} \quad x \in [0, 1],$$

Integration time: $T = 0.16$.

For this more severe shock tube problem, Fig. 5 shows the performance of non-staggered, staggered central and CWENO schemes at $T = 0.16$ with $N = 100$. Similar to the Sod's problem, non-staggered central scheme is as well as staggered central scheme. Our results show that non-staggered and staggered central schemes generate slightly oscillation near discontinuities. In the density profile shown in Fig. 5 (a), (a'), the non-staggered central scheme produces undershoots whereas, the staggered central scheme produces slightly overshoots. Also, non-staggered one gives better solution near discontinuities than CWENO in particular for the density profile of this Riemann problem.

Test 7 (Shock-entropy problem). In this test which is used by authors of [25] we solve the Euler equations (18) with a moving Mach = 3 shock interacting with sine waves in density, i.e.,

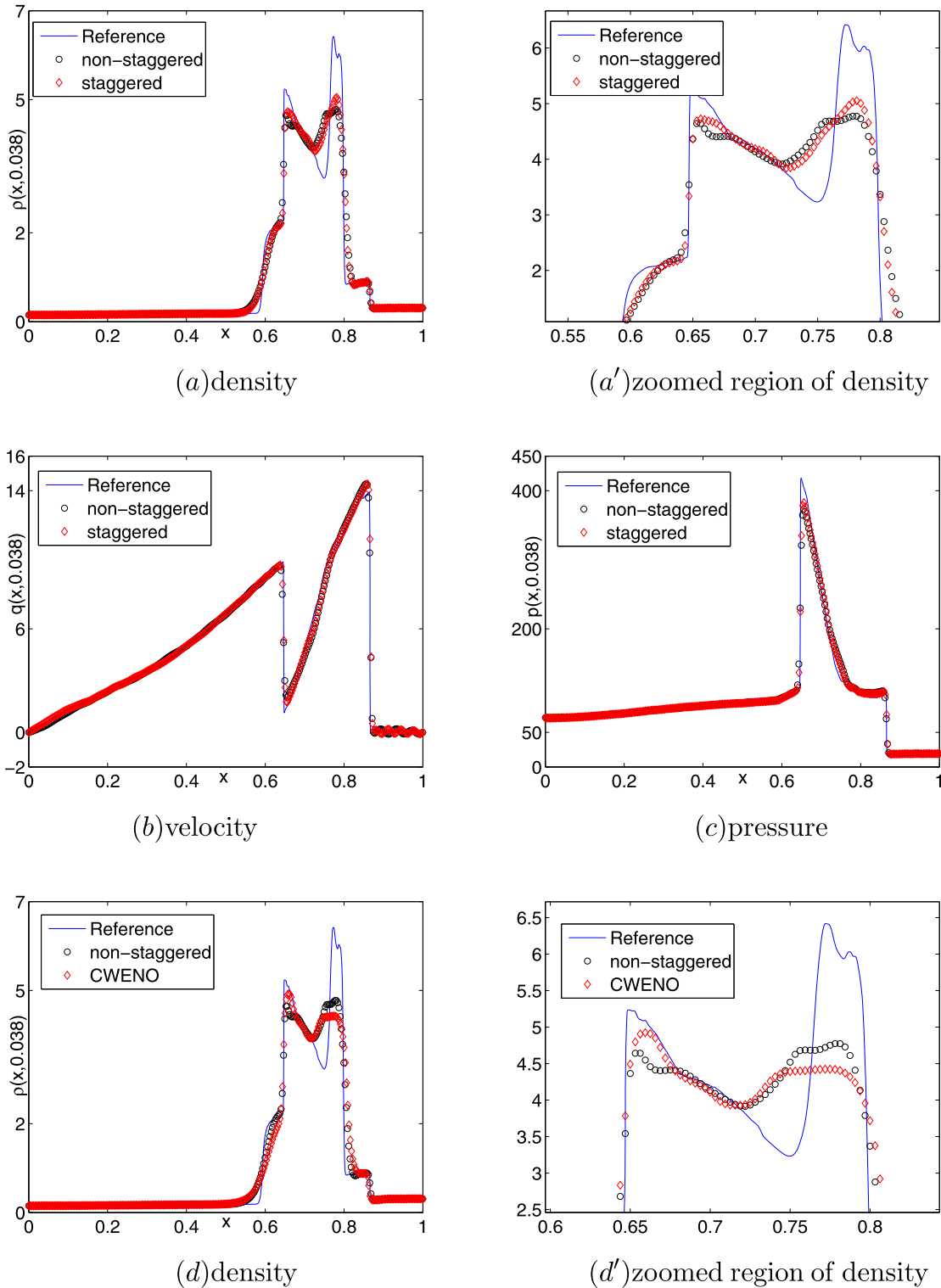


Fig. 7. Test 8 by $N = 320$ at $T = 0.038$.

$$u(x, 0) = \begin{cases} (3.85714, 10.1418096304, 39.16655928489427)^T, & -5 \leq x < -4, \\ (1 + 0.2 \sin(5x), 0, 2.5)^T, & -4 \leq x \leq 5, \end{cases}$$

$x \in [-5, 5]$,
Integration time: $T = 1.8$.

The flow contains physical oscillations which have to be resolved by the numerical methods. The “reference solution”, which is a converged solution computed by [20] with 2000 grid points. We test the performance of the staggered, non-staggered and CWENO schemes in smooth regions and the ability to capture shocks with $N = 200$. We show the numerical solutions of the density profile in Fig. 6 at $T = 1.8$. We note that the non-staggered central scheme

gives slightly better solution with respect to the staggered central scheme. Also, we observe in Fig. 6 that non-staggered is sharper than CWENO in particular for the density profile.

Test 8 (Woodward and Colella's problem). For the final test which is taken from the literature [27] we solve the Euler equations (18) with a shock interaction problem with solid wall boundary conditions, applied to both ends given by the initial data

$$u(x, 0) = \begin{cases} (1, 0, 2500)^T, & 0 \leq x < 0.1, \\ (1, 0, 0.025)^T, & 0.1 \leq x < 0.9, \\ (1, 0, 250)^T, & 0.9 \leq x \leq 1, \end{cases} \quad x \in [0, 1],$$

Integration time $T = 0.038$.

The computations are done, using $N = 320$, and the solution is displayed together with a “reference solution”, obtained by [20] with $N = 2560$. In Fig. 7 we show the density, the velocity, and the pressure at $T = 0.038$. We note that the non-staggered central scheme performs as well as the staggered central scheme. Also, Fig. 7 shows the performance of non-staggered and CWENO schemes. As is seen, the non-staggered scheme gives better solution than CWENO scheme.

5. Conclusion

In this work, we converted a fourth-order staggered central scheme introduced by Peer et al. [20] into fourth-order non-staggered central scheme. First, we would like to comment that this scheme can be easily generalized to 2D problems, using dimension-by-dimension reconstructions. We applied the non-staggered and staggered central schemes to several test problems. Numerical experiments show that non-staggered scheme is well comparable with the staggered scheme whereas the non-staggered scheme is very simple to be implemented. Also the non-staggered scheme has the non-oscillatory behavior as well as the staggered scheme and the desired accuracy. In general, the staggered scheme produces slightly better resolution for shocks than the non-staggered scheme. The fourth-order non-oscillatory non-staggered central scheme was extended for solving hyperbolic systems of conservation laws. Therefore we applied the non-staggered, staggered and CWENO schemes to Euler equations of gas dynamics. Numerical results demonstrate the staggered scheme produces slightly better resolution near the discontinuous. Also, the non-staggered central scheme gives better solution near discontinuities than CWENO scheme.

Acknowledgements

The authors would like to thank A.A.I. Peer for his valuable programming advise. The authors are very thankful to the reviewers for carefully reading the paper, their comments and suggestions have improved the quality of the paper.

References

- [1] J. Balbas, E. Tadmor, C.-C. Wu, Non-oscillatory central schemes for one- and two-dimensional MHD equations: I, *J. Comput. Phys.* 201 (2004) 261–285.
- [2] F. Bianco, G. Puppo, G. Russo, High-order central schemes for hyperbolic systems of conservation laws, *SIAM J. Sci. Comput.* 21 (1999) 294–322.
- [3] M. Dehghan, On the solution of an initial-boundary value problem that combines Neumann and integral condition for the wave equation, *Numer. Methods Partial Differential Equations* 21 (2005) 24–40.
- [4] M. Dehghan, Finite difference procedure for solving a problem arising in modeling and design of certain optoelectronic devices, *Math. Comput. Simulation* 71 (2006) 16–30.
- [5] M. Dehghan, Time-splitting procedures for the solution of the two-dimensional transport equation, *Kybernetes* 36 (2007) 791–805.
- [6] K.O. Friedrichs, P.D. Lax, Systems of conservation equations with a convex extension, *Proc. Natl. Acad. Sci.* 68 (1971) 1686–1688.
- [7] A. Harten, S. Osher, Uniformly high-order accurate nonoscillatory schemes, I, *SIAM J. Numer. Anal.* 24 (1987) 279–309.
- [8] S.K. Godunov, A finite difference method for the numerical computation of discontinuous solutions of the equations of fluid dynamics, *Mat. Sb.* 47 (1959) 271–290.
- [9] A. Kurganov, G. Petrova, A third-order semidiscrete genuinely multidimensional central scheme for hyperbolic conservation laws and related problems, *Numer. Math.* 88 (2001) 683–729.
- [10] A. Kurganov, E. Tadmor, New high-resolution central schemes for non-linear conservation laws and convection–diffusion equations, *J. Comput. Phys.* 160 (2000) 241–282.
- [11] G.S. Jiang, D. Levy, C.T. Lin, S. Osher, E. Tadmor, High-resolution nonoscillatory central schemes with nonstaggered grids for hyperbolic conservation laws, *SIAM J. Numer. Anal.* 35 (1998) 2147–2168.
- [12] G.S. Jiang, E. Tadmor, Nonoscillatory central schemes for multidimensional hyperbolic conservation laws, *SIAM J. Sci. Comput.* 19 (1998) 1892–1917.
- [13] P.D. Lax, Weak solutions of non-linear hyperbolic equations and their numerical computation, *Comm. Pure Appl. Math.* 7 (1954) 159–193.
- [14] D. Levy, G. Puppo, G. Russo, Central WENO schemes for hyperbolic systems of conservation laws, *Math. Model. Numer. Anal.* 33 (1999) 547–571.
- [15] D. Levy, G. Puppo, G. Russo, A fourth-order central WENO schemes for multi-dimensional hyperbolic systems of conservation laws, *SIAM J. Sci. Comput.* 24 (2002) 456–480.
- [16] D. Levy, G. Puppo, G. Russo, Compact central WENO schemes for multidimensional conservation laws, *SIAM J. Sci. Comput.* 22 (2000) 656–672.
- [17] X.D. Liu, S. Osher, Non-oscillatory high order accurate self-similar maximum principle satisfying shock capturing schemes I, *SIAM J. Numer. Anal.* 33 (1996) 760–779.
- [18] X.D. Liu, E. Tadmor, Third order nonoscillatory central scheme for hyperbolic conservation laws, *Numer. Math.* 79 (1998) 379–425.
- [19] H. Nessyahu, E. Tadmor, Non-oscillatory central differencing for hyperbolic conservation laws, *J. Comput. Phys.* 87 (1990) 408–463.
- [20] A.A.I. Peer, A. Gopaul, M.Z. Dauhoo, M. Bhuruth, A new fourth-order non-oscillatory central scheme for hyperbolic conservation laws, *Appl. Numer. Math.* 58 (2008) 674–688.
- [21] A.A.I. Peer, A. Gopaul, M.Z. Dauhoo, M. Bhuruth, New high-order ENO reconstruction for hyperbolic conservation laws, in: *Proceedings of the 2005 Conference on Computational and Mathematical Methods on Science and Engineering*, 2005, pp. 446–455.
- [22] J. Qiu, C.-W. Shu, On the construction, comparison, and local characteristic decomposition for the high order central WENO schemes, *J. Comput. Phys.* 183 (2002) 187–209.
- [23] G. Russo, Central schemes for conservation laws with application to shallow water equations, in: *Trends and Applications of Mathematics to Mechanics: STAMM 2002*, Springer-Verlag, 2005, pp. 225–246.
- [24] R. Sanders, A. Weiser, A high resolution staggered mesh approach for nonlinear hyperbolic systems of conservation laws, *J. Comput. Phys.* 101 (1992) 314–329.
- [25] C.W. Shu, S. Osher, Efficient implementation of essentially non-oscillatory shock-capturing schemes II, *J. Comput. Phys.* 83 (1989) 32–78.
- [26] G. Sod, A survey of several finite difference methods for systems of non-linear hyperbolic conservation laws, *J. Comput. Phys.* 27 (1978) 1–31.
- [27] P. Woodward, P. Ciella, The numerical solution of two-dimensional fluid flow with strong shocks, *J. Comput. Phys.* 54 (1988) 115–173.
- [28] Y.H. Zhran, Central ADER schemes for hyperbolic conservation laws, *J. Math. Anal. Appl.* 346 (2008) 120–140.
- [29] M. Zennaro, Natural continuous extensions of Runge–Kutta methods, *Math. Comp.* 46 (1986) 119–133.
- [30] A. Kurganov, A. Polizzi, Non-oscillatory central schemes for traffic flow models with arrhenius look-ahead dynamics, *Networks and Heterogeneous Media* 4 (3) (2009) 1–21.